

Fig.1. Spin j of resonances plotted against k , the N c.m. momentum.

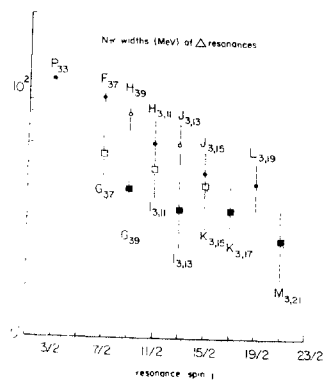


Fig.2. $N\bar{N}$ widths plotted against resonance spin j .

INVESTIGATION OF THE NATURE OF ENHANCEMENTS
OBSERVED IN $\Lambda\rho$ EFFECTIVE MASS SPECTRA
B.A.Shahbazian, P.P.Temnikov, A.A.Timonina,
A.M.Rozhdestvensky
JINR, Dubna

The inclusive $\Lambda\rho$ effective mass spectrum from the interactions of 7 GeV/c average momentum neutrons with carbon nuclei has been investigated. Four enhancements have been discovered in it.

The comparison of physical and experimental conditions at which these peaks have been observed in this and other experiments /1-3/, suggests that they should be the manifestations of peculiarities of the $\Lambda\rho$ elastic scattering and $\Lambda\Sigma$ - and $\Sigma\Lambda$ - conversion effective cross sections.

To analyze this hypothesis, a model of creation and interactions of Λ - and Σ - hyperons in carbon nuclei, bombarded with 7 GeV/c average momentum neutrons, has been developed.

The model proposed is based on impulse approximation, which is valid in our case firstly because the neutron energy considerably exceeds the nucleon binding energy in the carbon nucleus and secondly because we consider only the low mass part (2053.859 - 2553.859) MeV/c² (or the relative momentum interval $P_\Lambda = 0. - 2.0$ GeV/c) of the whole $\Lambda\rho$ effective mass spectrum which extends in this experiment up to ~ 4800 MeV/c².

The most important intranuclear cascade processes resulting in the $\Lambda\rho + (\text{Anything})$ and $\Lambda\rho\rho + (\text{Anything})$ final states, which form the statistical sample of this experiment, have been modelled. For this purpose all known experimental data on Λ - and Σ - hyperon production, their two-body interactions with nucleons and decay processes /1,4/ have been used. The geometrical and kinematical restrictions imposed by this experiment have been accounted for.

The expected smallness of the ratio of resonance widths to the difference of their masses permitted us to use the isolated resonances approximation ^{/5/}. For the same reasons and what is more, because the low energy and potential scattering amplitudes vary with the $\Lambda\rho$ effective mass in opposite ways, it turned out possible to neglect all interference terms.

Thus the $\Lambda\rho$ elastic scattering effective cross section has been expressed as a sum of four cross sections corresponding to the low energy scattering with scattering parameters

$a_s = a_t = a$ and $\tau_s = \tau_t = \tau$, elastic resonance scattering with parameters M_2, Γ_2 and M_3, Γ_3 and of the potential scattering. The last cross section has been assumed to be proportional to the two-body $\Lambda\rho$ phase space volume $R_2(M_{\Lambda\rho})$. Namely, $G_{\text{pot}}^{\Lambda\rho}(M_{\Lambda\rho}) = \pi R^2 R_2(M_{\Lambda\rho})$, where R is an average range of the $\Lambda\rho$ interaction forces. This experiment did not permit us to account for the elastic $\Lambda\rho$ scattering and $\Sigma\Lambda$ -conversion channels coupling effects. So the $\Lambda\Sigma$ - and $\Sigma\Lambda$ -conversion processes contributed independently of the elastic scattering. The least square analysis resulted in all above mentioned parameters and moreover the contributions A, B, C, D of the elastic $\Lambda\rho$ scattering, $\Lambda\Sigma$ - and $\Sigma\Lambda$ conversion processes as well as of the independent Λ and proton creation in intranuclear cascade processes. The results of fits presented in table I clearly show that the best fit parameters for the $\Lambda\rho$ effective mass spectrum fit ($M_{\Lambda\rho}$ -fit) do not differ significantly from those for simultaneous $\Lambda\rho$ effective mass spectrum and elastic scattering effective cross section fit $((M_{\Lambda\rho} + G_{\Lambda\rho}^{\text{eff}}) - \text{fit})$. We come to the following conclusions.

1. The analysis, performed in the frame of this model, permitted us to successfully

describe not only the $\Lambda\rho$ effective mass spectrum with its enhancements, i.e., the results of the $\Lambda\rho$ enhancement production experiment but also the behaviour of the $\Lambda\rho$ elastic scattering effective cross section in the Λ -hyperon relative momentum interval $P_\Lambda = (0.1-2.0)$ GeV/c, i.e., the results of the $\Lambda\rho$ enhancement formation experiments. This is demonstrated in Figs.1 and 2.

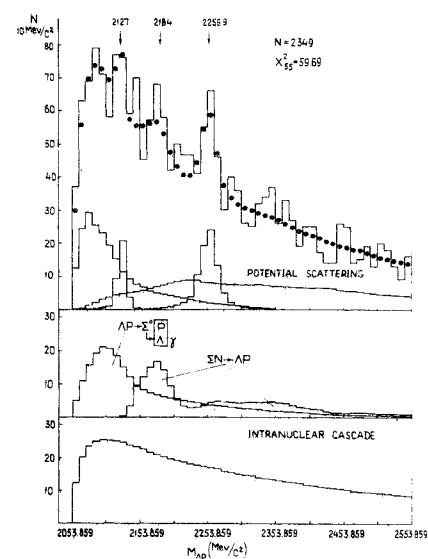


Fig. 1

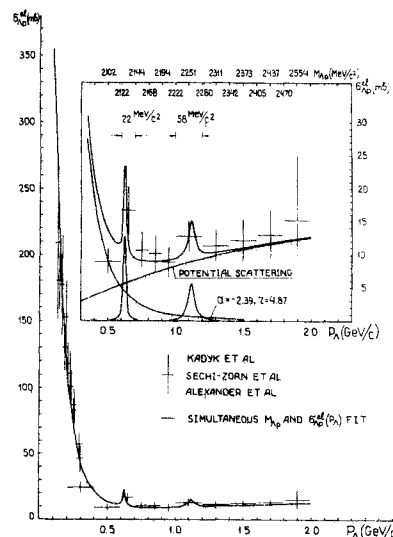


Fig. 2

2. The peak near the Λp threshold is due to the negative sign Λp scattering length effect at low energy. The negative scattering length excludes the possibility of the existence of (Λp) bound states. The unsuccessful up to now search for the Λ - hyperdeuteron confirms this result.

3. The peaks at $2127 \text{ MeV}/c^2$ and $2257 \text{ MeV}/c^2$ are due to the Λp elastic narrow resonances at $620 \text{ MeV}/c$ and $1120 \text{ MeV}/c$ of relative Λ hyperon momenta, respectively (fig.2).

4. The enhancement near $2184 \text{ MeV}/c^2$ is of kinematical origin and is due to the two-step process $n^{12}\text{C} \rightarrow (\Sigma N) + (\text{Anything})$, $\Sigma N \rightarrow \Lambda p$.

5. The average range of the Λp interaction forces is about 0.66 fm .

6. The components of the average polarization of Λ - hyperons, presumed to be daughters of Λp - systems along the beam direction ρ_z , normal to the Λp -production plane - ρ_y and normal to both these directions - ρ_x , are zero within the limits of errors.

7. It is shown that all these results are very stable with respect to considerable changes of the Λp - and ΣN - c.m.s. angular distributions used to model various processes.

The neglect of interference terms in the expressions for the Λp scattering effective cross section, as well as the assumption $\Gamma_{tot} \approx \Gamma_\ell \approx \Gamma_R$ and the use of the isolated resonance approximation, are justified due to the narrowness of the resonance widths and the total precision of this experiment (Table 1, IVth col.).

8. It is shown that light nuclei, carbon nucleus at least, could be used as high density nucleon targets to study low energy scattering of unstable particles on nucleons in the absence of monoenergetic beams of such particles.

9. With the increase of the atomic number of nuclei one can expect the wearing perhaps even disappearing of enhancements because of the increasing probability of rescattering in heavy nuclei.

10. The effective cross sections of the observed Λp resonances have been estimated: $\sigma_{\Lambda p}^d (620) = 12.80 \text{ mb}$, $\sigma_{\Lambda p}^d (1120) = 5.61 \text{ mb}$ (fig.2).

The authors are indebted to prof. A.M. Bal'din for the continuous interest and support of this work.

Table 1
The results of fitting

	$M_{\Lambda p} + \sigma_{\Lambda p}^{ef}$ - fit $M_{\Lambda p} + \sigma_{\Lambda p}^{ef}$ - fit	$(M_{\Lambda p} + \sigma_{\Lambda p}^{ef})$ - fit for isotropic c.m.s. distributions over $\cos \theta_{\Lambda \Lambda}, \cos \theta_{\Lambda \Sigma},$ $\cos \theta_{\Sigma \Lambda}$
χ^2_n	$\chi^2_{34} = 34.39$	$\chi^2_{55} = 59.69$
C.L. (%)	44.92	31.56
		$\chi^2_{55} = 59.57$
χ^2_{55}		31.92
$a (\text{fm})$	-2.30 ± 0.35	-2.39 ± 0.04
$r (\text{fm})$	4.73 ± 0.50	4.87 ± 0.05
$M_2 (\text{MeV}/c^2)$	2126.30 ± 1.66	2127.00 ± 3.38
$\Gamma_2 (\text{MeV}/c^2)$	3.78 ± 0.92	3.76 ± 0.96
$M_3 (\text{MeV}/c^2)$	2256.40 ± 3.12	2256.90 ± 1.33
$\Gamma_3 (\text{MeV}/c^2)$	15.97 ± 4.40	15.55 ± 4.20
$A(\Lambda p \rightarrow \Lambda p)$	0.332 ± 0.008	0.336 ± 0.005
$B(\Lambda p \rightarrow \Sigma p)$	0.117 ± 0.005	0.109 ± 0.003
$C(\Sigma \Lambda)$	0.081 ± 0.004	0.083 ± 0.004
$D(i.c.b.)^*$	0.469 ± 0.004	0.471 ± 0.005
$R (\text{fm})$	0.656 ± 0.020	0.664 ± 0.015

* i.c.b. - intranuclear cascade background.

REFERENCES

1. B.A. Shahbazian et al. Physics of Elementary Particles and Atomic Nuclei, v.4, part 3, 811 (1973); Nucl. Phys., B53, 19 (1973); Lett. Nuovo Cim., 6, 63 (1973); JINR, Dubna, EL-7669, 1974.
2. Tai Ho Tan. Phys. Rev. Lett., 23, 395 (1969); D.T. Cline et al. Phys. Rev. Lett., 20, 1452 (1968); D. Eastwood et al. Phys. Rev., D3, 2603 (1971).

3. J.T. Read et al. Phys. Rev., 165, 1495 (1968).
 4. J.A. Kadyk et al. Nucl. Phys., B27, 13 (1971);
 G. Alexander et al. Phys. Rev., 173, 1452 (1968);
 B. Sechi-Zorn et al. Phys. Rev., 175, 1735 (1968);
 O. Benary et al. A Compilation of YN Reactions, UCRL-20000 YN (1970).
 5. G. Breit. Theory of Resonance Reactions and Allied Topics Handbuch der Physik, Band XL 1/1 S.1, Springer-Verlag, 1959.

KN SCATTERING AND THE PROBLEM OF THE
 $S \rightarrow 1$ BARYON RESONANCES

G. Giacomelli

Istituto di Fisica dell'Università di Bologna, Italy
 Istituto Nazionale di Fisica Nucleare, Sezione di Bologna

1. Introduction

This report will summarize the present situation on low energy KN scattering and will discuss in particular the following contributions to this conference:

1. BART coll.: Quasi two-body K^+N interactions below 1.5 GeV/c (1);
2. BART coll.: Phase shift analysis of $K^+p \rightarrow K^+\Delta$ below 1.5 GeV/c (2);
3. BICGR coll.: Study of $K^+p \rightarrow K^0p$ in $1490 < E_{cm} < 1700$ MeV (3);
4. BP coll.: Angular distribution for the $K^+p \rightarrow K^0p$ in $1600 E_{cm} 1900$ MeV; (4)
5. PNL Measurement of $K^+n \rightarrow K^+p$ at 0.7, 0.8 and 0.9 GeV/c (5).

Low energy KN scattering data have been discussed in terms of phase shift analyses of various complexity. We shall limit our considerations to the simplest ones, using the phase shift analyses as a method for searching for resonant states and/or for the parametrization of the experimental data.

Fig. 1. Total, elastic and inelastic cross sections in $I = 1$ and $I = 0$ (1).
 The curves are hand drawn through the experimental points.

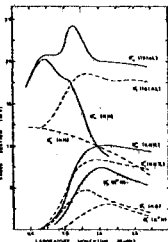


Fig. 1 (1) illustrates the present knowledge on low energy K^+N scattering in both $I = 1$ and $I = 0$ states: the K^+p total cross section has an asymmetric structure at a lab. momentum of 1.25 GeV/c. The structure arises from a slowly varying elastic cross section and the opening up of inelastic channels, dominated by the $K^+p \rightarrow K^+\Delta^{++}$. The structure may thus be thought to be a threshold effect for the $K^+\Delta$ channel.

The K^+N , $I = 0$ total cross section has a shoulder at 0.8 GeV/c and a peak at 1.15 GeV/c. The shoulder corresponds to a peak in the elastic cross section, while the peak at 1.15 GeV/c is connected to the opening up of the $K(890)N$ channel.

The isospin structure of the various elastic channels is:

$$K^+p \rightarrow K^+p \quad Z_1 \quad (1)$$

$$K^+n \rightarrow K^+n \quad \frac{1}{2}(Z_1 - Z_0) \quad (2)$$

$$K^+n \rightarrow K^+p \quad \frac{1}{2}(Z_1 + Z_0) \quad (3)$$

$$K^+p \rightarrow K^0p \quad \frac{1}{4}(Z_0 + Z_1 - 2Y_1) \quad (4)$$

where Z_1 , Z_0 denote the strangeness +1, isospin 1 and 0 amplitudes, while Y_1 denotes the strangeness -1, isospin 1 amplitude.

2. $K^+p \rightarrow K^+p$

The amount of data available on K^+p elastic scattering is quite large and of good accuracy (6). No new data have been presented at this conference. It would be nice to have measurements of the F -parameter at $0.5 + 0.8$ GeV/c and some measurements of the A and R parameters. (7)

The most recent phase shift analyses go to 2.5 GeV/c and use many theoretical refinements. The analyses agree qualitatively, but there are quantitative disagreements. For instance at 0.8 GeV/c there are differences of up to a factor of two on the contribution of the $P_{1/2}$ cross section; the behaviour of the S-wave is not too well determined at high momenta.

It has been remarked long time ago (8) that the K^+p amplitudes are very similar to the background amplitudes in π^+p after the resonance contribution has been removed. In particular the behaviour of the $P_{1/2}$ amplitude, which has an appearance similar to a small resonance loop, is approximately reproduced in the π^+p amplitudes.

3. $K^+p \rightarrow K^0\Delta$

One of the difficulties connected with the study of the 1.25 GeV/c structure via the elastic scattering is its large inelasticity. One may thus hope to obtain new information from the study of the main inelastic channel in this energy region

$$K^+p \rightarrow K^+\Delta^{++}(1423) \quad L \rightarrow \pi^+p \quad (5)$$

The detailed analysis of (5) involves considerable difficulties of practical and theoretical nature: the amount of data for reaction (5) is neither as abundant nor as accurate as that for the elastic reaction. All data come from bubble chamber experiments and have typical statistics of 500 events per angular distribution. Fig. 2 shows the integrated cross sections computed with the empirical interference model and with the P-wave interference model; the two calculations differ by about 30% at the higher energies.